Separation Science and Technology
Publication details, including instructions for authors and subscription information:
http://www.informaworld.com/smpp/title~content=t713708471

Removal of Iron from Water Using Adsorbent Carbon

Regina de F. P. M. Moreira[a]; Vivian S. Madeira[a]; Humberto J. José[a]; E. Humeres[b]
[a] Departamento de Engenharia Química e Engenharia de Alimentos, Universidade Federal de Santa Catarina, Florianópolis, SC, Brazil [b] Departamento de Química, Universidade Federal de Santa Catarina, Florianópolis, Brazil

Online publication date: 08 July 2010

To cite this Article Moreira, Regina de F. P. M. , Madeira, Vivian S. , José, Humberto J. and Humeres, E.(2005) 'Removal of Iron from Water Using Adsorbent Carbon', Separation Science and Technology, 39: 2, 271 — 285
To link to this Article: DOI: 10.1081/SS-120027558
URL: http://dx.doi.org/10.1081/SS-120027558

SEPARATION SCIENCE AND TECHNOLOGY
Vol. 39, No. 2, pp. 271–285, 2004

Removal of Iron from Water Using Adsorbent Carbon

Regina de F. P. M. Moreira,[1,*] Vivian S. Madeira,[1] Humberto J. José,[1] and E. Humeres[2]

[1]Departamento de Engenharia Química e Engenharia de Alimentos and [2]Departamento de Química, Universidade Federal de Santa Catarina, Campus Universitário—Trindade, Florianópolis, Brazil

ABSTRACT

A novel adsorbent carbon to remove iron from water was evaluated. Bench scale and pilot scale tests were performed to characterize the mechanism of the iron removal. The adsorption equilibrium of iron removal can be described using the Langmuir isotherm, assuming a monolayer. In the absence of dissolved oxygen, Fe^{2+} is adsorbed on the solid surface as a monolayer of 62.7×10^{-3} mat-g·g^{-1}, while the monolayer of oxidized iron coverage in the air-equilibrated system is 72.7×10^{-3} mat-g·g^{-1}. The iron removal results from the adsorption of oxygen followed by the oxidation of Fe^{2+} catalyzed by the adsorbent

*Correspondence: Regina de F. P. M. Moreira, Departamento de Engenharia Química e Engenharia de Alimentos, Universidade Federal de Santa Catarina, Campus Universitário—Trindade, 88040-670 Florianópolis, SC, Brazil; Fax: 55-048-331-9687; E-mail: regina@enq.ufsc.br.

DOI: 10.1081/SS-120027558 0149-6395 (Print); 1520-5754 (Online)

carbon surface. The Fe^{3+} precipitates on the solid, forming a hydrated iron oxide-coated carbon that is also able to adsorb iron. The kinetics of iron removal was modeled using the film and pore diffusion model. Pilot tests performed with and without pre-aeration showed results similar to those observed on the bench scale.

Key Words: Adsorbent carbon; Iron removal; Water; Kinetics.

INTRODUCTION

Iron and manganese are natural constituents of the Earth's crust, and both elements create serious esthetic problems in drinking water supplies. The removal of ferrous iron (Fe^{2+}) from groundwater has been generally achieved by simple aeration, or the addition of an oxidizing agent, followed by rapid sand filtration.[1]

It has been demonstrated that the use of iron oxide-coated sand is effective in the removal of iron[2,3] and also in the removal of uncomplexed metals cations (Cu, Cd, Pb, Ni, Zn)[4] and certain oxyanionic metals (SeO_3, AsO_3).[4,5] In this case, the iron removal from water involves the adsorption of Fe^{2+} onto the surface of the filter media and the subsequent oxidation of adsorbed Fe^{2+} in the presence of dissolved oxygen to regenerate the adsorption site for continuation of the process.[3] The applications of iron-coated sand are influenced by the coating techniques, and the type of iron oxide coating produced depends on the physical and chemical environments in which the iron oxide is prepared and coated.[5]

Active carbon can also be used for the removal of iron from water. A mechanism of iron removal was recently proposed by Rönnholm et al.[6] in which the active carbon acts as a catalyst. The oxidation is presumed to proceed on the active carbon surface, where oxygen is dissociatively adsorbed. Fe^{2+} ions donate an electron to the adsorbed oxygen, which reacts with a hydronium ion forming a surface hydroxyl and releasing a water molecule (Fig. 1). Synergetic effects are expected when using adsorbents that are able to oxidize Fe^{2+} and to form an iron oxide-coated solid.

The objective of this work was to verify the capacity of iron removal using a specially treated subbituminous coal,[7] which from now on will be referred to as adsorbent carbon (AdC), to be used in the treatment of water with a high iron content.

MARCEL DEKKER, INC.
270 Madison Avenue, New York, New York 10016

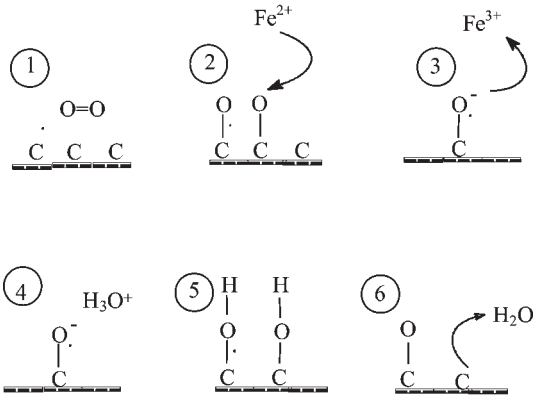

Figure 1. Mechanism of Fe^{2+} oxidation on carbon surface.[6]

EXPERIMENTAL PART

Materials

Stock solutions of $FeSO_4$ and $FeCl_3$ (Merck, p.a., Rio de Janeiro, Brazil) were used in bench studies at concentrations in the range 10 to 900 $\mu mol\,L^{-1}$. In pilot and full-scale studies, groundwater with a total iron concentration in the range of 0 to 180 $\times\ 10^{-3}$ mat-g$\cdot L^{-1}$ (mili-atom gram per liter) was used.

The adsorbent carbon investigated (AdC) was a subbituminous coal from Santa Catarina State (Brazil). This material was crushed into 1.65-mm diameter particles. The adsorbent carbon was washed with distilled water to remove adhered small particles and used without any further treatment. A commercial activated carbon (AcC) (Carbomafra, Brazil) was used to compare the efficiency of iron removal.

The surface area and textural characterization were determined in a BET surface area measuring device (Autosorb-1, Quantachrome, Florida, USA). All other characterization parameters were evaluated according to standard methods (ASTM or ABNT).

Bench Tests

The equilibrium of iron removal on carbon adsorbent was performed using the static method, stirring (at 50 rpm) 100 mL of 10×10^{-3} to 900×10^{-3} mat-g$\cdot L^{-1}$ Fe^{2+} or Fe^{3+}solutions with 1.0 g of solid. After

MARCEL DEKKER, INC.
270 Madison Avenue, New York, New York 10016

24 hours, the concentration of total iron and Fe^{2+} in the reminiscent solution was determined using the 1,10 phenanthroline method in a Hach DR2000 spectrophotometer.[8] Control flasks were submitted to the same conditions without adsorbent carbon. The tests were performed under air-equilibrated and N_2-equilibrated systems. In the N_2-equilibrated system, deoxygenated water was used to prepare the aqueous solution of $FeSO_4$ and N_2 (White Martins, 99.99% pure, Joinville, Brazil) was bubbled through the flasks for 24 hours to prevent Fe^{2+} oxidation.

The amount of iron removed was determined by a mass balance, Eq. (1)

$$q_t = \frac{(C_{Feo} - C_{Fet})^* V}{W} \tag{1}$$

where V is the volume of solution, W is the mass of adsorbent carbon, and C_{Feo} and C_{Fet} are the initial and final total iron concentrations.

The kinetics of iron removal was performed by contacting 2 g of adsorbent carbon and 200 mL of 89.5×10^{-3} mat-g·L^{-1} Fe^{2+} solution. Samples of solution were taken every 30 min and analyzed for total iron concentration.

Pilot Scale Tests

The pilot plant used in this work is schematically shown in Fig. 2. It is able to treat 150 L/h of groundwater and consists of a pre-aerator and an adsorbent carbon column. Two series of tests were performed. In the first series, the groundwater was pumped directly into the adsorbent carbon column, without pre-aeration. In the second series, the groundwater was pre-aerated before being passed through the adsorbent carbon column.

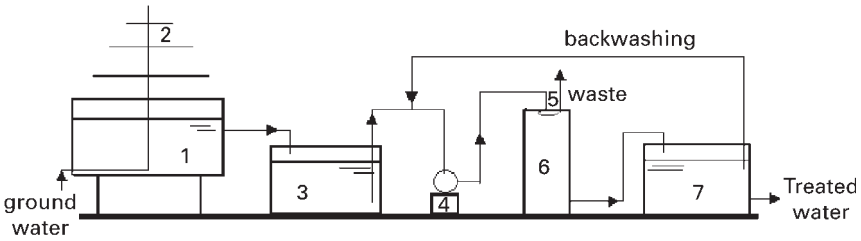

Figure 2. Flowsheet of the pilot plant [1. Tank (500 L); 2. Pre-aerator; 3. Tank (250 L); 4. Pump; 5. Dispositive for selection filtration or backwashing; 6. AdC column; 7. Tank (500 L)].

MARCEL DEKKER, INC.
270 Madison Avenue, New York, New York 10016

SEM/EDAX Analysis

Scanning electron microscopy/energy dispersive x-rays were performed using a SEM/EDAX, Philips XL-30 Scanning Electronic Microscope. Elemental microprobe and elemental distribution mapping techniques were used to analyze the elemental constitution of solid samples. The scanning energy for EDAX analysis was from 0 to 10.23 keV with an elapsed time of 100 s.

RESULTS AND DISCUSSION

Textural Characterization

The porous structure of the AdC was characterized from low-temperature (77 K) adsorption isotherms of nitrogen (Fig. 3).

Although the volume of N_2 adsorbed at 77 K is low, the shape of the isotherm is typical of mesoporous solids, which frequently show closed-loop hysteresis in the P/Po range 0.4 to 1.0. Hysteresis occured because the mechanism of adsorption in the mesopores was different from that of the desorption, and the type

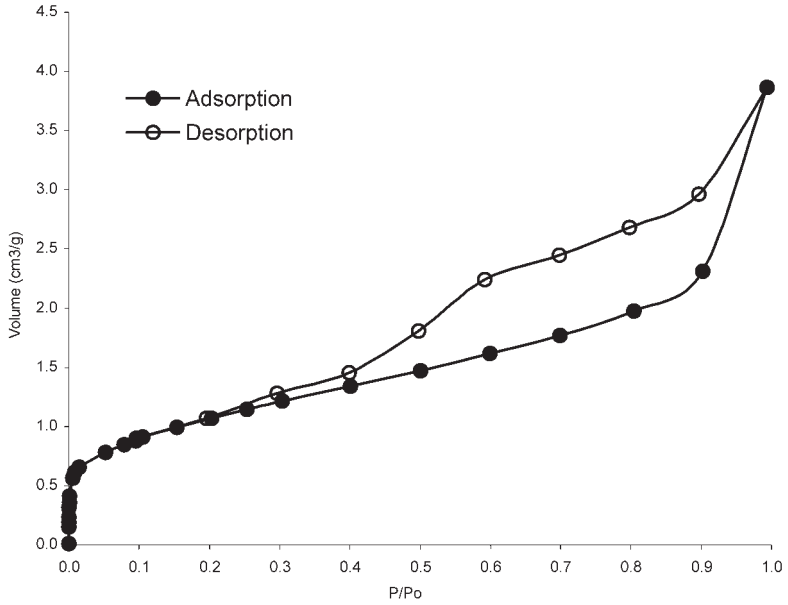

Figure 3. Adsorption of N_2 on adsorbent carbon at 77 K.

MARCEL DEKKER, INC.
270 Madison Avenue, New York, New York 10016

presented by the adsorbent carbon was of slit-shaped pores.[9] The low adsorption volume is a consequence of the small surface area of the solid.

The analysis of micropores was performed using the Dubinin–Radushkevich (DR) equation[9] (Fig. 4). The microporous volume calculated by the DR equation was very low ($V_{\text{micropores}} = 2.53 \times 10^{-3}\,\text{cm}^3/\text{g}$) in comparison to other activated carbons.[9]

The complete characterization of the adsorbent carbon is shown in Table 1. This adsorbent carbon is a mineral coal with a high ash content, and the point of zero charge was at nearly neutral pH. The zero charge condition is suitable to oxidize and precipitate Fe^{3+}.[4] The characteristics of the AdC and commercial activated carbon (AcC) were different, especially with respect to the surface area. The AdC was neither treated thermally nor activated and, therefore, the cost of its use would be much lower than that of the AcC.

Equilibrium of Adsorption

Figure 5 shows the equilibrium of adsorption of total iron on the adsorbent carbon, at 25°C in the air-equilibrated and N_2-equilibrated systems.

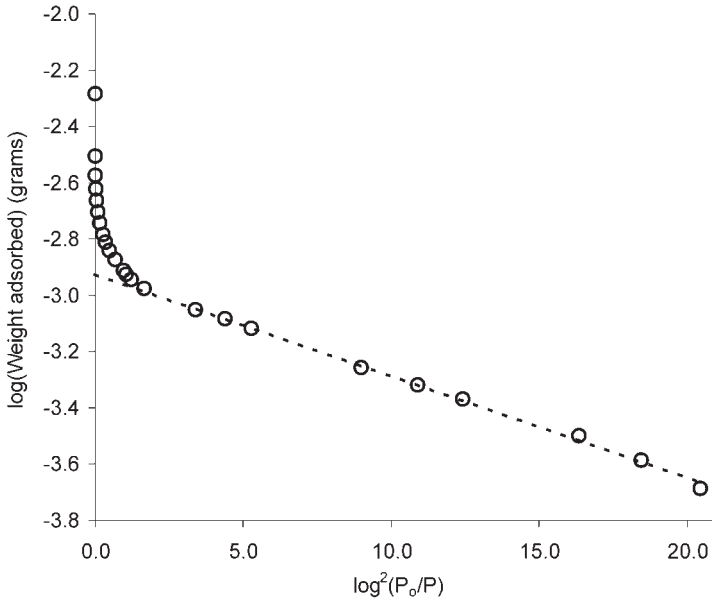

Figure 4. DR plot for the adsorbent carbon.

MARCEL DEKKER, INC.
270 Madison Avenue, New York, New York 10016

Table 1. Characterization of adsorbent and activated carbon.

Parameter	AdC	AcC	Method
Solubility in HCl, %	2.68	—	NBR 14234
Solubility in NaOH, %	1.18	—	NBR 14234
True density, g/cm^3	1.64	1.44	NBR 14234
Effective diameter, mm	1.65	1.68	NBR 14234
Uniformity coefficient	0.36	—	NBR 14234
Iodine number, mg/g	$<$40.5	—	ASTM D 4607-94
Phenol index, g/L	1.30	—	MB-3411
pH_{pzc}	6.5–7.5	9.7	Streat & Rangel-Mendez[18]
BET surface area, m^2/g	3.8	1228.1	N_2 adsorption
Elemental analysis, %			
C	47.3	—	
H	3.3	—	
N	1.0	—	
O	5.1	—	
S	1.5	—	
Ash content, %	41.8	8.7	ASTM 2866-94
Porosity, %	19.4	—	Mercury porosimeter

It can be observed that the Langmuir equation, Eq. (2), suitably fits the experimental data in both air and N_2 systems.

$$q_e = \frac{q_m \cdot bC_e}{1 + bC_e} \tag{2}$$

where q_e is the concentration of iron in the solid (mat-g$\cdot$g^{-1}), C_e is the concentration of total iron in aqueous solution (mat-g$\cdot$L^{-1}), q_m is the monolayer covering the solid surface (mat-g$\cdot$g^{-1}), and b is the adsorption equilibrium constant (L$\cdot$mat-g^{-1}).

In the N_2 equilibrated system, the removal of iron can be ascribed only to adsorption of Fe^{2+} on the solid's surface due to the absence of oxygen in the medium. No Fe^{3+} was measured in the aqueous solution in absence of dissolved oxygen, as also observed by Rodríguez-Reinoso et al.[10] for the iron oxidation catalyzed by commercial activated carbon. The adsorption equilibrium constant b (Table 2) was significantly different from that found in the air-equilibrated system, as expected from the previous adsorption of oxygen followed by the oxidation of Fe^{2+} and precipitation of Fe^{3+}.

Besides adsorption, the observed iron removal in the air-equilibrated system results from the oxidation and precipitation of Fe^{3+} on the adsorbent carbon surface, since the adsorbent carbon catalyzes the oxidation of Fe^{2+} as

Marcel Dekker, Inc.
270 Madison Avenue, New York, New York 10016

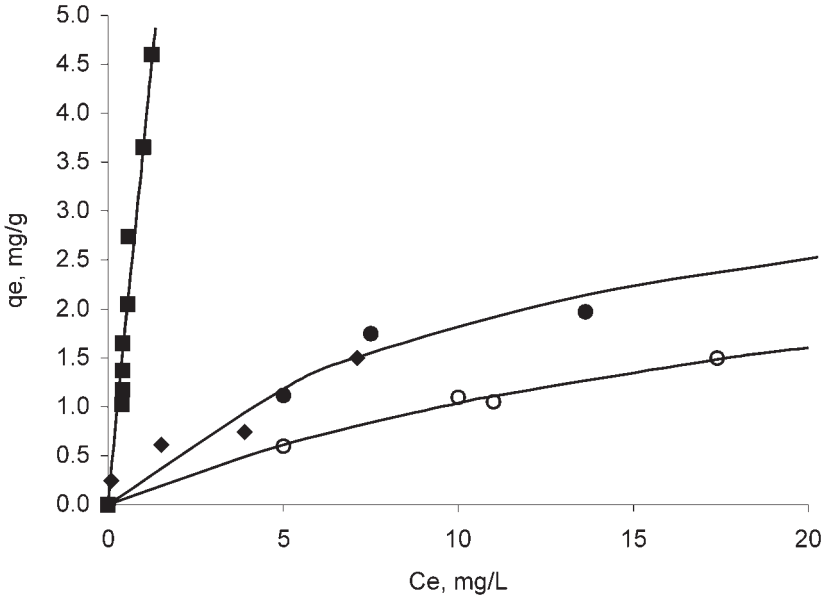

Figure 5. Equilibrium adsorption of total iron on adsorbent carbon in air-equilibrated and N_2-equilibrated systems, at 25°C. ● AdC-air-equilibrated using Fe^{2+}; ○ AdC-N_2-equilibrated using Fe^{2+}; ◆ AdC-air-equilibrated using Fe^{3+}; ■ AcC-air-equilibrated using Fe^{2+}.

proposed by Rönnhom et al.,[6] and at a pH that is near neutral, the Fe^{3+} aqua species precipitates.[4] The iron oxide coverage also removes the iron from aqueous solution through a similar mechanism proposed for the iron oxide-coated sand.[2,3]

It is noteworthy that the iron removal observed for AcC compared to AdC by unit of mass was comparatively high because of its greater surface area.

Table 2. Langmuir equilibrium constants for iron removal in aqueous solution at 25°C.

	AdC		AcC
	Air equilibrated	N_2 equilibrated	Air equilibrated
b, L·mat-g^{-1}	4.58	2.35	57.13
q_m, mat-g·g^{-1}	72.7×10^{-3}	62.7×10^{-3}	3958×10^{-3}
q_m, mat-g/m^2	19.1×10^{-3}	16.5×10^{-3}	3.22×10^{-3}

Marcel Dekker, Inc.
270 Madison Avenue, New York, New York 10016

However, when the iron removal is expressed by surface area unit, AdC presents a higher iron removal than AcC (see Table 2).

The iron removal equilibrium of Fe^{3+} is also shown in Fig. 5. No difference was observed between Fe^{2+}/air-equilibrated and Fe^{3+}/air-equilibrated system, supporting the assumption that the main mechanism of iron removal is the deposition of Fe^{3+} on the solid's surface.

The scanning electronic microscopy of AdC and saturated-AdC is shown in Fig. 6. Virgin solid has a very rough surface, and cracks, macropores, or roughness can be found on the AdC surface. On the other hand, saturated-AdC appears with a uniformly coated surface. The iron concentration in the solid, measured by EDAX analysis, shows an enrichment in iron and oxygen, resulting from the precipitation of hydrated iron oxide on the solid (Table 3).

Figure 6(c) shows, in detail, an aggregate particle with higher iron concentration than in the rest of the particle. A high sulfur concentration, indicating the presence of pyrite, was also measured.

Kinetics of Iron Removal on Bench Scale

Noncatalytic oxidation of Fe^{2+} occurs spontaneously in a solution containing dissolved oxygen. The time required for uncomplexed ferrous iron to undergo oxidation to the ferric state depends on several factors, such as the pH, temperature, amount of dissolved oxygen, and presence of other soluble ions. The lower the pH and temperature, the longer the time required for completion of the oxidation reaction.[11]

In the presence of a heterogeneous catalyst such as carbon, the oxidation reaction is very fast and the rate-limiting step of the kinetics of iron removal becomes the mass transfer from the solution to the solid particle. The kinetic of iron removal was established using the film and pore diffusion model[12–14] assuming spherical particles. This model was derived under the assumption of both no surface diffusion and local adsorption equilibrium inside the particle.

The mass balance in the liquid phase can be written as Eq. (3)

$$\frac{dC}{dt} = -\frac{3vk_f}{RV_L}(C - C_{i\ r=R}) \tag{3}$$

where C is the bulk concentration of iron in liquid phase, C_i is the concentration of iron inside the particle, R is the radius of the particle, k_f is the mass-transfer coefficient in the film around the particle, v is the volume of solid, V_L is the volume of solution, and t is the time.

Marcel Dekker, Inc.
270 Madison Avenue, New York, New York 10016

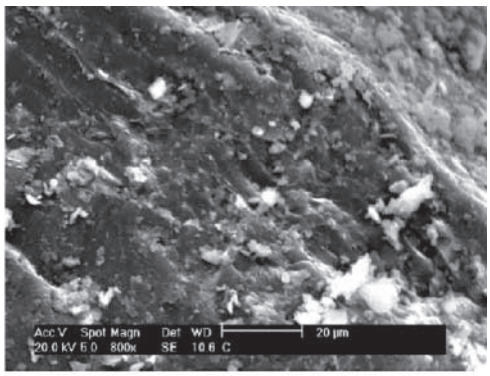

(a)

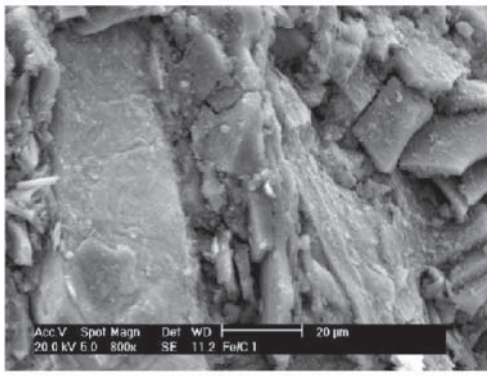

(b)

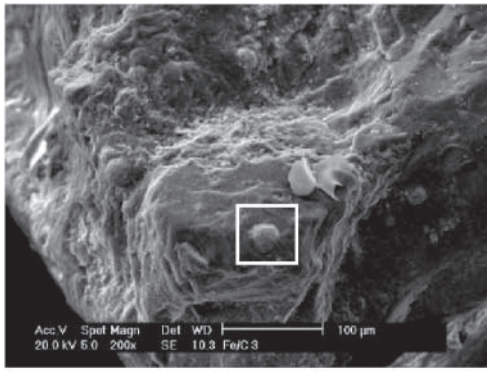

(c)

Figure 6. SEM solids before and after iron removal in aqueous solution: (a) virgin; (b) saturated AdC; and (c) saturated AdC detail.

Table 3. EDAX analysis of different carbons.

	Non-used AdC		Used AdC		Used AdC detail	
Element	% weight	% atomic	% weight	% atomic	% weight	% atomic
C	74.70	82.36	36.80	51.76	33.6	52.27
O	16.56	13.71	25.04	26.44	21.16	24.71
Al	3.20	1.57	13.38	8.38	4.10	2.84
Si	4.17	1.96	18.03	10.84	4.44	2.95
K	0.56	0.19	3.77	1.63	0.51	0.24
Ti	0.33	0.09	0.92	0.32	1.35	0.53
Fe	0.48	0.11	2.06	0.62	15.51	5.19
S	ND	ND	ND	ND	19.34	11.27

Note: ND, nondetectable.

The mass balance inside the particle is described by Eq. (4)

$$(\varepsilon_p + \rho_{app} f'(C_i)) \frac{\partial C_i}{\partial t} = D_{ef} \left(\frac{\partial^2 C_i}{\partial r^2} + \frac{2}{r} \frac{\partial C_i}{\partial r} \right) \tag{4}$$

where

$$f'(C_i) = \frac{q_m b}{(1 + bC_i)^2} \tag{5}$$

and ε_p is the particle porosity, q_i is the iron concentration in the solid phase, ρ_{app} is the apparent density, and D_{ef} is the effective diffusivity. Equation (4) was solved using the boundary conditions given by Eqs. (6) to (8):

$$t = 0 \quad C_i = 0 \tag{6}$$

$$r = 0 \quad \left(\frac{\partial C_i}{\partial r} \right) = 0 \tag{7}$$

$$r = R; \quad \frac{\partial C_i}{\partial r} = \frac{k_f}{D_{ef}} (C_b - C_i) \tag{8}$$

A computational program was developed to solve Eqs. (3) to (8) and to predict the decrease of total iron concentration with time. The necessary parameters to simulate the adsorption rate are the coefficient of mass transfer in the film around the particles (k_f) and the effective diffusion coefficient inside the particles (D_{ef}). The experimental kinetic data of adsorption of total iron on adsorbent carbon and the calculated curve are shown in Fig. 7. The experimental data were fitted with $k_f = 4.0 \times 10^{-4}$ cm/min and $D_{ef} = 6.0 \times 10^{-6}$ cm^2/min. The effective diffusion coefficient (D_{ef}) is of the same order

Marcel Dekker, Inc.
270 Madison Avenue, New York, New York 10016

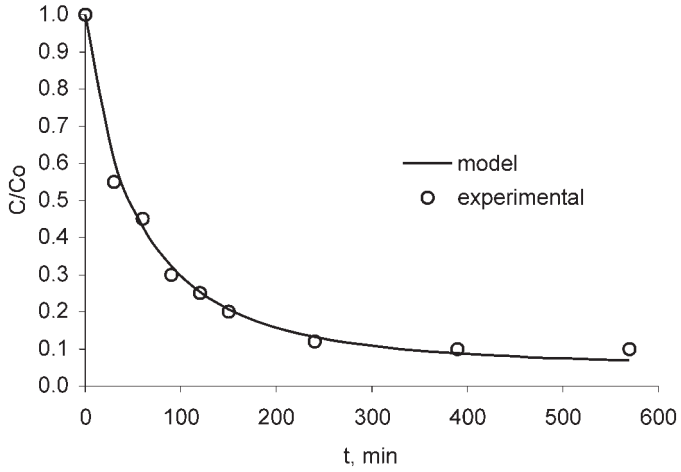

Figure 7. Kinetics of iron removal at 25°C in air equilibrated system at 50 rpm; mass of AdC: 2.0 g; C_{Feo}: 89.5×10^{-3} mat-g·L^{-1}.

of magnitude as it for the adsorption of various metal ions on other adsorbent carbons.[15]

The initial rate of adsorption was fast and the equilibrium was achieved in about 10 hours. The Biot number ($Bi = k_f \cdot D_p/D_{ef}$) is about 11, and indicates that mass transfers both through the film and inside the particle are important in determining the rate of adsorption.[16]

Tests on Pilot Scale Without Pre-aeration

A pilot plant containing 35 kg of adsorbent carbon in a fixed bed was used to treat groundwater with 70 to 110 $\times 10^{-3}$ mat-g·L^{-1} of iron. When the total iron in the effluent of the filter reached 5.37×10^{-3} mat-g·L^{-1} (limit concentration for drinking water), the system was submitted to backwashing with treated water ($C_{Fe} < 0.18 \times 10^{-3}$ mat-g·L^{-1}). Two adsorption cycles were performed and the results are shown in Fig. 8 and Table 4.

Table 4 shows the high efficiency of total iron removal from the groundwater (88% in the first cycle and 75% in the second cycle). Despite this result, Fig. 8 shows that the quality of treated water is not within the standard limit for drinking water ($<5.37 \times 10^{-3}$ mat-g·L^{-1}). The amount of dissolved oxygen in groundwater is very low, and the catalytic oxidation of Fe^{2+} is insufficient, as was shown previously in the test of iron removal in absence of dissolved oxygen (see Fig. 5).

MARCEL DEKKER, INC.
270 Madison Avenue, New York, New York 10016

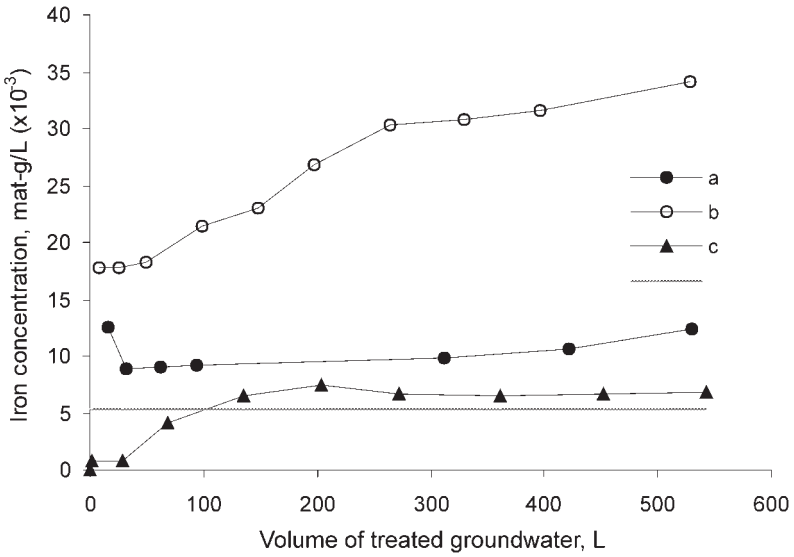

Figure 8. Outlet total iron concentration of treated groundwater on pilot scale. (a) First cycle without pre-aeration: initial iron concentration: 78.6×10^{-3} mat-g $\cdot$ L^{-1}; retention time: 6 min; (b) second cycle, without pre-aeration: initial iron concentration: 108.9×10^{-3} mat-g $\cdot$ L^{-1}; retention time: 12 min; and (c) first cycle, after pre-aeration: initial iron concentration: 107.1×10^{-3} mat-g $\cdot$ L^{-1}; retention time: 8 min; dashed lines represent the maximum limit (5.4×10^{-3} mat-g $\cdot$ L^{-1}).

Tests on Pilot Scale After Pre-aeration

A pre-aerator was installed in the pilot plant as recommended by Boyd and Watten.[17] Analysis of total iron and Fe^{2+} showed that only 14% of total iron was oxidized after this pre-aeration. Figure 8(c) and Table 5 show that the

Table 4. Experimental conditions in first and second cycle of iron removal on pilot scale without pre-aeration.

	First cycle[a]	Second cycle[a]
C_{Fe} inlet, mat-g $\cdot$ L^{-1}	78.8×10^{-3}	109.2×10^{-3}
C_{Fe} outlet, mat-g $\cdot$ L^{-1}	8.95×10^{-3}	26.86×10^{-3}
Flow rate, L $\cdot$ min^{-1}	3.3	1.65
Retention time, min	6	12
Percentage iron removal	88	75

[a]Mass of adsorbent: 35 kg.

MARCEL DEKKER, INC.
270 Madison Avenue, New York, New York 10016

Table 5. Experimental conditions of pilot test after pre-aeration.

C_{Fe} inlet, mat-g/L	103.8×10^{-3}
C_{Fe} outlet, mat-g/L	$\sim 5.37 \times 10^{-3}$
Mass of adsorbent carbon, kg	35
Flow rate, $L \cdot min^{-1}$	2.28
Retention time, min	8
Percentage iron removal	95

concentration of total iron in the effluent of the filter is always near to the maximum limit.

CONCLUSION

Iron removal by adsorbent carbon can be explained by considering the oxidation of Fe^{2+} by the adsorbed oxygen on the solid's surface. Fe^{3+} precipitates on the surface forming a hydrated, iron oxide-coated carbon that is also capable of removing the iron.

The equilibrium of iron removal can be described by the Langmuir isotherm. The kinetics of iron removal is fast and the equilibrium can be achieved in about 10 hours. The film and pore mass transfer kinetic model is suitable to describe the kinetics of adsorption. It shows that both the external and internal mass transfer are important in determining the kinetics of iron removal.

Tests on a pilot scale show that it is necessary to pre-aerate the groundwater to increase the dissolved oxygen and to allow the Fe^{2+} oxidation catalyzed by the adsorbent carbon.

REFERENCES

1. Aziz, H.; Smith, P. The influence of pH and coarse media on manganese precipitation from water. Water Res. **1992**, *26*, 853–855.
2. Sharma, S.K.; Mendis, B.S.; Greetham, M.R.; Schippers, J.C. Modelling adsorptive iron removal in filters. Water Supply **2000**, *18*, 604–608.
3. Sharma, S.K.; Kappelhof, J.; Groenendijk, M.; Schippers, J.C. Comparison of physicochemical iron removal mechanisms in filters. J. Water SRT—Aqua **2001**, *50*, 187–198.
4. Benjamin, M.M.; Sletten, R.; Bailey, R.P.; Bennett, T. Sorption and filtration of metals using iron-oxide-coated sand. Water Res. **1996**, *30*, 2609–2620.

MARCEL DEKKER, INC.
270 Madison Avenue, New York, New York 10016

5. Lo, S.L.; Chen, T.Y. Adsorption of Se(IV) and Se(VI) on an iron-coated sand from water. Chemosphere **1997**, *35*, 919–930.
6. Rönnholm, M.R.; Wärna, J.; Valrakari, D.; Salmi, T.; Laine, E. Kinetics and mass transfer effects in the oxidation of ferrous sulfate over doped active carbon. Catalysis Today **2001**, *66*, 447–452.
7. INPI (Instituto Nacional de Propriedade Intelectual), P10304474-2, "Método para tratamento de água ferruginosa e/ou manganosa," 2003.
8. *DR 2000 Spectrophotometer Instrument Manual*; Hach Company, 1994; 223–228.
9. Marsh, H. *Activated Carbon Compendium*; Elsevier Science, 2001.
10. Rodríguez-Reinoso, F.; Ahumada, E.; Lizama, H.; Orellana, F.; Suárez, C.; Huidobro, A.; Sepulveda-Escribano, A. Catalytic oxidation of Fe(II) by activated carbon in the presence of oxygen. Effect of the surface oxidation degree on the catalytic activity. Carbon **2002**, *40* (15), 2827–2834.
11. Cotton, F.A.; Wilkinson, G. *Advanced Inorganic Chemistry—A Comprehensive Text*; John Wiley & Sons: New York, 1980.
12. McKay, G.; Al-Duri, B. Comparison of theory and application of several mathematics models to predict kinetics of single component batch adsorption systems. Trans. IChemE **1990**, *68* (Part B), 225–233.
13. Moreira, R.F.P.M.; Peruch, M.G.B.; Kunhen, N.C. Adsorption of reactive dyes onto granular activated carbon. Latin. Am. Appl. Res. **1998**, *28* (1/2), 37–41.
14. Moreira, R.F.P.M.; Soares, J.L.; José, H.J.; Rodrigues, A.E. The removal of reactive dyes using high-ash char. Braz. J. Chem. Eng. **2001**, *18* (3), 327–336.
15. Xiu, G.-H.; Li, P. Prediction of breakthrough curves for adsorption of lead (II) on activated carbon fibers in a fixed bed. Carbon **2000**, *38*, 975–981.
16. Ruthven, D.M. *Principles of Adsorption and Adsorption Process*; John Wiley & Sons: New York, 1984.
17. Boyd, C.; Watten, B. Aeration systems in aquaculture. Rev. Aquat. Sci. **1989**, *1* (3), 425–472.
18. Streat, M.; Rangel-Mendez, J.R. Adsorption of cadmium by activated carbon cloth: influence of surface oxidation and solution pH. Water Res. **2002**, *36*, 1244–1252.

Received November 2002
Revised April 2003